Acknowledgments

We would like to express our gratitude to all the authors who have contributed to this book with so much enthusiasm.

We are much indebted to our colleague Prof. Dr. Eelco Bergsma who has been the coauthor of this book, spending much time with us and exhibiting so much patience while completing the digital workup of the book, thereby making this work possible.

Yvette Braaksma-Besselink and Dr. Hinke Marijke Jellema, orthoptists: we would like to thank you both for your contribution and insightful information on the intriguing aspects of diplopia.

Dr. Carl-Peter Cornelius: thank you so much for the enthusiastic elaboration on so many aspects of the anatomy of the orbit and the exceptional accompanying illustrations. It has been a great pleasure working with you.

This book would not be complete without your expertise and extensive input.

Prof. Dr. Thomas Dodson: your participation has been an honor. Though from a far distance, we are grateful for your Seattle University of Washington contribution. Thomas, your membership in the Peer Review Group is much respected.

Prof. Dr. Eddy Becking and Prof. Dr. Jonathan Roos: also thanks to you for being on board of the Peer Review Group.

Dr. Gertjan Mensink and Dr. Rob Noorlag: it has been a pleasure to work with you on the topic of orbital cellulitis.

Dr. Bram van der Pol and Dr. Geert-Jan Rutten: thank you for the neurosurgical input on the highly specialized area of orbital roof fractures.

Prof. Dr. Wilmar Wiersinga: as an internationally well-respected endocrinologist with a special interest in patients with Graves' disease, your contribution to the etiology and management of this disease is invaluable.

Dr. Maartje de Win: your contribution on imaging aspects is much appreciated; it is an indispensable and essential part of diagnostics, planning, and control in orbital trauma and pathology. We would also like to thank Roel Kloos, ophthalmologist at the department of Ophthalmology of the Amsterdam University Medical Centers for sharing many figures in several chapters.

To my fellow colleagues of the Dutch "Orbit Team" of the Amsterdam University Medical Centers, location AMC. Prof. Dr. Leander Dubois, Prof. Dr. Eddy Becking, Dr. Ruud Schreurs, Prof. Dr. Thomas Maal, Dr. Jesper

Jansen, and Juliana Sabelis, we are very grateful for all the work you have done with the emphasis on “teamwork.” You have supplied this book with important issues on the current workup of the patient with an orbital wall fracture as well as with detailed information on treatment aspects including the preoperative digital planning concept.

We would like to thank Karthik Periyasamy of the Springer Editorial team for the continuous and structural support during the creation of the book.

We appreciate the financial support to realize this book by the scientific organization of the Dutch Association of Oral and Maxillofacial Surgery: Bevordering Bijzondere Wetenschappelijke Onderwijs en Onderzoekactiviteiten BOOA. We also want to thank the MKA-Groep, The Netherlands for their financial support.

A special word of thanks to all the patients referred to in this book.

Without your input, there would be no such book.

Peter J. J. Gooris

Maarten P. Mourits

Contents

Contributors

Alfred G. Becking, MD, DDS, PhD., FEBOMFS Department of Oral and Maxillofacial Surgery, Amsterdam University Medical Centers, Location AMC, Amsterdam, The Netherlands

J. Eelco Bergsma, MD, DDS, PhD Department of Oral and Maxillofacial Surgery, Amphia Hospital Breda, Breda, The Netherlands

Amsterdam University Medical Centers, Location AMC, Amsterdam, The Netherlands

Acta dental school, Amsterdam, The Netherlands

Yvette Braaksma-Besselink Department of Ophthalmology, Amsterdam University Medical Centers, Location AMC, Amsterdam, The Netherlands

Carl-Peter Cornelius, MD, DDS Department of Oral and Maxillofacial Surgery, Facial Plastic Surgery, Ludwig Maximilians University, Munich, Bavaria, Germany

Jasjit K. Dillon, MD, DDS, BDS, FDSRCS Department of Oral and Maxillofacial Surgery, University of Washington, Seattle, WA, USA

Oral and Maxillofacial Surgery Harborview Medical Center, University of Washington, Seattle, WA, USA

Thomas Dodson, DMD, MPH, FACS Department of Oral and Maxillofacial Surgery, University of Washington, Seattle, WA, USA

Leander Dubois, MD, DDS, PhD Department of Oral and Maxillofacial Surgery, Amsterdam University Medical Centers, Amsterdam, The Netherlands

Peter J. J. Gooris, MD, DDS, PhD, FEBOMFS Department of Oral and Maxillofacial Surgery, Amphia Hospital Breda, Breda, The Netherlands

Amsterdam University Medical Centers, Amsterdam, The Netherlands

Department of Oral and Maxillofacial Surgery, University of Washington, Seattle, WA, USA

Jesper Jansen, MD, DDS, PhD Department of Oral and Maxillofacial Surgery, Amsterdam University Medical Centers, Amsterdam, The Netherlands

Hinke Marijke Jellema, PhD Department of Ophthalmology, Amsterdam University Medical Centers, Location AMC, Amsterdam, The Netherlands

Thomas J. J. Maal, PhD, MSc 3D Lab Department of Oral and Maxillofacial Surgery, Radboud University Medical Center, Nijmegen, The Netherlands

Gertjan Mensink, MD, DDS, PhD Department of Oral and Maxillofacial Surgery, Amphia Hospital Breda, Breda, The Netherlands

Maarten P. Mourits, MD, PhD Amsterdam University Medical Centers, Location AMC, Amsterdam, The Netherlands

Rob Noorlag, MD, DDS, PhD Department of Oral and Maxillofacial Surgery, University Medical Center Utrecht, Utrecht, The Netherlands

Bram van der Pol, MD Department of Neurosurgery, St. Elisabeth-Tweesteden Hospital Tilburg, Tilburg, The Netherlands

J. Roos, MD, PhD Department of Ophthalmology, University of Milan and Mario Negri Institute, Milan, Italy

Geert-Jan Rutten, MD, PhD Department of Neurosurgery, St. Elisabeth-Tweesteden Hospital Tilburg, Tilburg, The Netherlands

Juliana F. Sabelis 3D Lab Department of Oral and Maxillofacial Surgery, Amsterdam University Medical Centers, Amsterdam, The Netherlands

Ruud Schreurs, MSc, PhD 3D Lab Department of Oral and Maxillofacial Surgery, Amsterdam University Medical Centers, Amsterdam, The Netherlands

Wilmar M. Wiersinga, MD, PhD Department of Internal Medicine-Endocrinology, Amsterdam University Medical Centers, Location AMC, Amsterdam, The Netherlands

Maartje M. L. de Win, MD, PhD Department of Radiology and Nuclear Medicine, Amsterdam University Medical Centers, Amsterdam, The Netherlands

Part I

Introduction

1 The Orbit: Introduction to "CrossRoads". Multidisciplinary Versus Solo Approach in Complex Cases

Maarten P. Mourits, Peter J. J. Gooris, and J. Eelco Bergsma

Already in 1920, in a report to the UK Minister of Health, the concept of team-based care was conceived [1]. Now, PubMed shows no less than 61,496 hits when one searches for "multidisciplinary." This short chapter is certainly not a plea to approach each and every medical problem by a team of specialists, but in cross-disciplinary caseload, today interdisciplinary care is mandatory. As we will see, when, for example, treating patients with Graves' disease, a multidisciplinary approach is highly recommended [2, 3].

Pathology in and around the orbit is typically an area where many medical disciplines intersect: ophthalmology, oral and maxillofacial surgery, ENT, plastic surgery, and endocrinology. Despite the expertise of every single specialist, tunnel vision is a threat and can lead to misdiagnosis.

With the introduction of medical specialists from different fields working closely together, this tendency for tunnel vision is coming to an end. In 1994, Stoll et al. [4] argued that "orbital complications of various pathogenesis" are best treated by interdisciplinary teamwork. The advantage of working with a multidisciplinary team will equate to a superior outcome for the patient: The end result of that input is much more than the sum of its parts. Also, the multidisciplinary consultation hour can serve as a real goldmine for the participating doctors during which much can be achieved. In order for this system to work effectively, each doctor needs to maintain their knowledge and associated skills by treating a minimum number of patients annually.

In the Netherlands, every doctor is allowed to perform any medical treatment, provided he/she does it according to the rules of the current "medical art"

In the Amphia Hospital in Breda, Netherlands, we have set up a collaboration between oral and maxillofacial surgeons, endocrinologists, and ophthalmologists. Over the past 15 years, this has proved to be very beneficial in treating ocular-related pathology. Our main focus has been Graves' orbitopathy and orbital fractures, but

M. P. Mourits (✉)
Amsterdam University Medical Centers, Location AMC, Amsterdam, The Netherlands

P. J. J. Gooris
Department of Oral and Maxillofacial Surgery, Amphia Hospital Breda, Breda, The Netherlands

Amsterdam University Medical Centers, Amsterdam, The Netherlands

Department of Oral and Maxillofacial Surgery, University of Washington, Seattle, WA, USA

J. E. Bergsma
Department of Oral and Maxillofacial Surgery, Amphia Hospital Breda, Breda, The Netherlands

Amsterdam University Medical Centers, Amsterdam, The Netherlands

Acta dental school, Amsterdam, The Netherlands

P. J. J. Gooris et al. (eds.), *Surgery in and around the Orbit*,
https://doi.org/10.1007/978-3-031-40697-3_1

related problems often revealed themselves during collaboration.

For those doctors who pursue the same goal as we have or those who are interested in both orbital surgery and ophthalmic orbital pathology, we hope our book "CrossRoads" is a valuable resource. It is not our aim to give a full description of all diseases, disorders, and treatments that exist in these fields; however, we have tried to provide an overview of some of the problems we have encountered and, hence, raise the interest for further reading.

References

1. Watkins J, Straughton K, King N. There is no 'I' in team but there may be a PA. Future Healthc J. 2019;6:177–80.
2. Bogusiak K, Puch A, Arkuszewski P. Goldenhar syndrome: current perspectives. World J Pediatr. 2017;13:405–15.
3. Wiersinga WM. Management of Graves' ophthalmopathy. Nat Clin Pract Endocrinol Metab. 2007;3:396–404.
4. Stoll W, Busse H, Wessels N. Detailed results of orbital and optic nerve decompression. NHO. 1994;42:685–90.

Part II

Anatomical Aspects of the Orbit

2 Anatomy of the Orbit: Overall Skeletal and Topographical Configuration

Carl-Peter Cornelius and Peter J. J. Gooris

Learning Objectives

To acquire a/an

- Comprehensive knowledge of the bony composition within and around the precincts of the orbits.
- Understanding of the topographical relationships of the orbit to the middle cranial fossa, cavernous sinus, infratemporal and pterygopalatine fossa, the paranasal air sinuses, and the lateral nasal wall.
- Impression of the individual variability of passageways in and out the orbit, which becomes specifically apparent in large-scale data pools of morphometric imaging (CT, MRI, CBCT) studies.
- Habitude for a thorough diagnostic workup to anticipate anatomic normal-variants for increased finesse in surgical planning and postoperative analysis.

C.-P. Cornelius (✉)
Department of Oral and Maxillofacial Surgery, Facial Plastic Surgery, Ludwig Maximilians University, Munich, Bavaria, Germany
e-mail: peter.cornelius@med.uni-muenchen.de

P. J. J. Gooris
Department of Oral and Maxillofacial Surgery, Amphia Hospital Breda, Breda, The Netherlands

Amsterdam University Medical Centers, Amsterdam, The Netherlands

Department of Oral and Maxillofacial Surgery, University of Washington, Seattle, WA, USA

Introduction

The orbits are paired mirror symmetric cavities of bone on either side of an intermediary compartment that is made up by the external and inner nose as well as the ethmoid and sphenoid sinuses. The orbits contain the eyeballs, i.e., the optical and light/image processing units, that represent the entry of the visual organ. Besides the eyeballs or globes with their refractive apparatus and retinal receptors, the visual organ consists of auxiliary adnexa, such as the lacrimal system, the extraocular muscles, and the adipose body including a multitude of neural connections and vascular supply. The posterior end of each orbital cavity (orbital apex) centers over the bony surfaces in the close vicinity of the superior orbital fissure and the posterior sinkhole of the inferior orbital fissure. These apex areas of the orbit are identical with the regions in juxtaposition of the lateral surfaces of the cubic body of the sphenoid bone. This coincidence fostered the idea of this fundamental anatomy chapter to describe the osseous construction of the orbits systematically building up from scratch at the orbital apex in the manner of a technical blueprint and exploded view drawings of the individual components. This process will result in a depiction of the overall assembly of both orbits and an outline of their spatial and topographical relationships at the transition between the maxillae, central and lateral midface components, and the cranial base

P. J. J. Gooris et al. (eds.), *Surgery in and around the Orbit*,
https://doi.org/10.1007/978-3-031-40697-3_2

and vault. Finally, the position, shape, dimensions, and important variations of the gates and passageways within this framework of bones and paranasal sinuses are addressed.

Method

Classic textbook and atlas descriptions were used to model the basic bony anatomy of the orbit and serve as introduction to outline the details of the passageways as well as topographical aspects. The recent relevant literature on the bony openings was identified and a small selection assigned to review the details of the bony openings. Photographs of post mortem human subject dissections, illustrations and digital drawings were synthesized to present a comprehensive survey of topics spanning the breadth of current knowledge on the bony constituents inside and around the orbit.

I. Osteology—Bony Building Blocks

Overall Skeletal and Topographical Configuration

The orbits are formed by facial and cranial bones. Each orbit is assembled of seven bones: sphenoid, frontal ethmoid, lacrimal, palatine, maxilla, zygoma [1]. These skeletal building blocks outline a cone- or pear-shaped cavity with a thick marginal rim framing the aperture at its base in contrast to the thin-walled cone construction. In terms of a geometric concept, the orbit can be translated into a pyramid with a quadrangular base, giving rise to four concentric walls which carry a three-sided spire or apex on the top end (Fig. 2.1a–f). The open base or aditus orbitae is projecting fronto-laterally and the apex posteromedially toward the optic foramen. The aditus is framed by thick and prominent marginal rims. These are well defined except for the medial side, which is discontinuous due to the interposition of the fossa for the lacrimal sac between its lower and upper part.[1] The medial rim or nasal orbital margin consists of the frontonasal process of the maxilla, the lacrimal bone, and the maxillary process of the frontal bone. The frontonasal process extends upward into the anterior lacrimal crest and forms the medial orbital margin in the lower part (MOMLP). The supraorbital rim continues into the posterior lacrimal crest in a more backward plane and creates a second parallel bone ridge, the upper part of the medial orbital margin (MOMUP) with the lacrimal fossa in between at a fluted bevel. The superior and inferior orbital margins curve distinctly posterior, so that the lateral rim is least projecting in the whole orbital circumference. The four walls of the human orbit or the internal orbit, respectively, are formed by the seven bones named above. The roof of the orbit is composed largely of the orbital plate of the frontal bone anteriorly and of the lesser wing of the sphenoid (LWS) with a minor part in the posterior part. The triangular shape of the roof narrows toward the orbital apex. The anterior portion of the frontal bone is containing the frontal sinuses which can extend far up into the squamous part of the frontal bone and far back over the orbital roof when extremely pneumatized. The floor of the anterior cranial fossa forms the endocranial side of both orbital roofs. The fossa for the lacrimal gland is a shallow depression in the anterolateral aspect of the roof next to the zygomaticofrontal suture (ZFS). A small depression in the anteromedial portion of the roof, the trochlear fovea, is the site of attachment for the fibrocartilaginous ring (pulley) girdling the tendon of the superior oblique muscle.

The junctions of the walls in the superomedial, superolateral, inferolateral, and inferomedial quadrants or pyramidal corners are rounded in reality. The overall configuration of the internal orbit (i.e., the inside) comes closer to the pyramid model than the external orbit due to its integration into frames, pillars, support, and pneumatized paranasal structures. With regard to their anatomical subunits, the entire orbital margin is occasionally divided into three sections, a supraorbital rim, an inferomedial or maxillary rim, and an inferolateral or zygomatic rim.

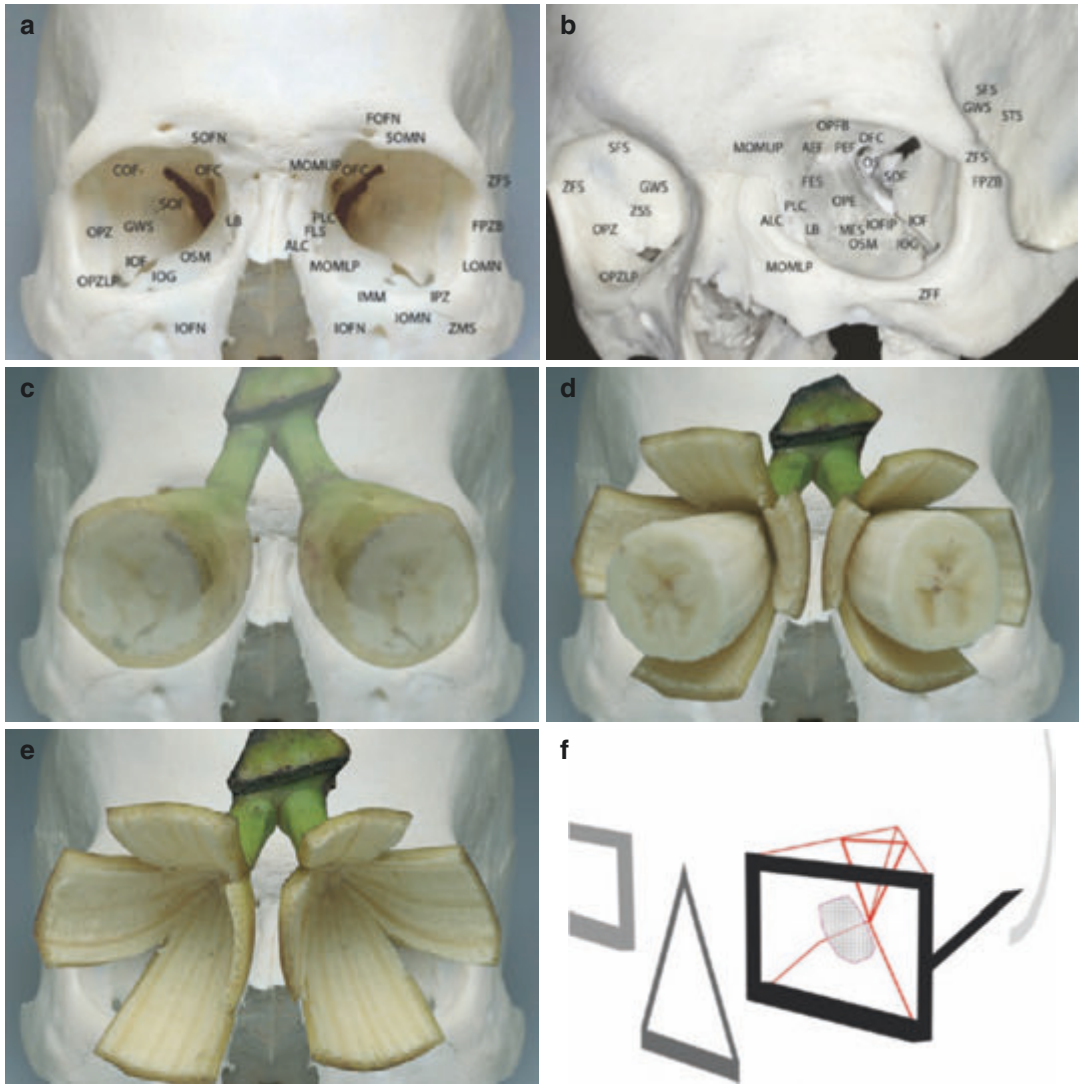

Fig. 2.1 (**a**) Orbits—anterior view—rim circumference. The broad blending of the anterior and posterior lacrimal crest results in discontinuity and ambiguity at the medial orbital rim. The anterior view limits the visibility over the internal orbital surfaces. *ALC* anterior lacrimal crest, *COF* cranioorbital foramen, *FLS* fossa for lacrimal sac, *FOFN* frontal orbital foramen/notch, *FPZB* frontal process of zygomatic bone, *GWS* greater wing of sphenoid, *IMM* infraorbital margin of maxilla, *IOMN* infraorbital margin, *IOF* inferior orbital fissure, *IOFN* infraorbital foramen, *IOG* infraorbital groove, *IPZ* infraorbital process of zygoma, *LB* lacrimal bone, *LOMN* lateral orbital margin, *MOMLP* medial orbital margin—lower part, *MOMUP* medial orbital margin—upper part, *OFC* optic foramen/canal, *OPLZP* orbital plate of zygoma lower part, *OPZ* orbital plate of zygoma, *OSM* orbital surface of maxilla, *PLC* posterior lacrimal crest, *SOF* superior orbital fissure, *SOFN* supraorbital foramen/notch, *SOMN* supraorbital margin, *ZFS* zygomatico–frontal suture, *ZMS* zygomatico—maxillary suture. (**b**) Orbits—left antero-oblique view to get insight into the inferomedial and anterolateral orbital walls concurrently. *AEF* anterior ethmoidal foramen, *FES* frontoethmoidal suture, *IOFIP* IOF isthmus promontory, *MES* maxilloethmoidal suture line, *OPE* orbital plate of ethmoid, *OPFB* orbital plate of frontal bone, *OS* optic strut, *PEF* posterior ethmoidal foramen, *PLC* posterior lacrimal crest, *SFS* sphenofrontal suture, *STS* spheno—temporal suture, *ZFF* zygomaticofacial foramen, *ZSS* zygomaticosphenoid suture. (**c–e**) Banana visualization of the geometric concept—both orbits. Likewise pealing bananas, the complex 3D orbital walls are translated into a 2D structure (Idea: C. P. Cornelius, Realization: Klaus Völcker, Regensburg). (**f**) Geometric scheme of the orbit—a quadrangular pyramid converts into a tetrahedron posteriorly. Accordingly, the frontal cross section in the apex is triangular. Dot matrix = posteromedial bulge (With permission from Orbital Fractures ISBN 0-88937-139-3 and ISBN 3-8017-(now Hogrefe Publishing), www.hogrefe.com)

Sphenoid Bone—Constituent of the Upper, Medial, and Lateral Orbital Wall

The sphenoid bone with its cuboidal body at the center and three pairs of outstretched wings or leg-like processes, respectively, can be appreciated as the principial constructive element of the skull base. It has often been considered as the most complex polymorphous bone of the human skeleton (Figs. 2.2a–d and 2.3).

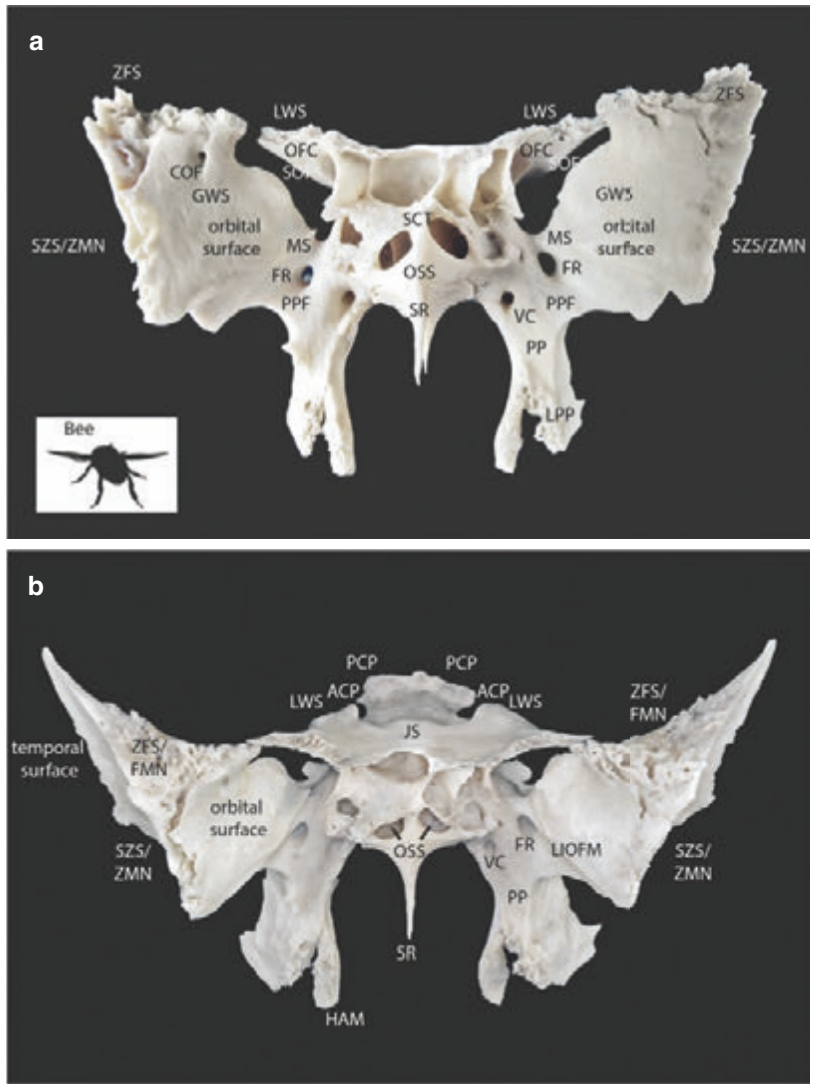

Fig. 2.2 Main features of the sphenoid from different aspects (**a**–**d**). The apices of the orbit are identical with the bony core regions around the SOF on both sides of the sphenoid body. (**a**) Sphenoid—anterior view—inset lower left corner: flying insect or bee like appearance. Note: 'Posterior ethmoid air cells' invading the upper anterior surface of the sphenoid body – correlating to 'Onodi' cells. *FR* foramen rotundum, *LPP* lateral pterygoid plate, *LWS* lesser wing of sphenoid, *MS* maxillary strut, *OSS* opening of sphenoid sinus, *PP* pterygoid process, *PPF* pterygopalatine fossa, *SR* sphenoid rostrum, *SZS/ZMN* sphenozygomatic suture/zygomatic margin, *VC* vidian canal/pterygoid canal. (Bee inset with permission from https://surgeryreference.aofoundation.org). (**b**) Sphenoid—Superoanterior view. *ACP* anterior clinoid process, *PCP* posterior clinoid process, *HAM* hamulus, *JS* jugum sphenoidale/sphenoid yoke, *LIOFM* lateral inferior orbital fissure margin, *SR* sphenoid rostrum, *ZFS/ZMN* zygomaticofrontal suture/zygomatic margin. (**c**) Sphenoid—Superior view—Inset lower left corner: flying bat like appearance. *CAG* carotid artery groove, *DS* dorsum sellae, *FO* foramen ovale, *FSM* foramen spinosum, *HF* hypophyseal fossa, *SQM* squamous margin. (Bat inset with permission from https://surgeryreference.aofoundation.org). (**d**) Sphenoid—Posterior view. *DS* dorsum sellae, *GLO* groove in the lateral orbit, *LPP* lateral pterygoid plate, *PCS* prechiasmatic sulcus, *PF* pterygoid fossa

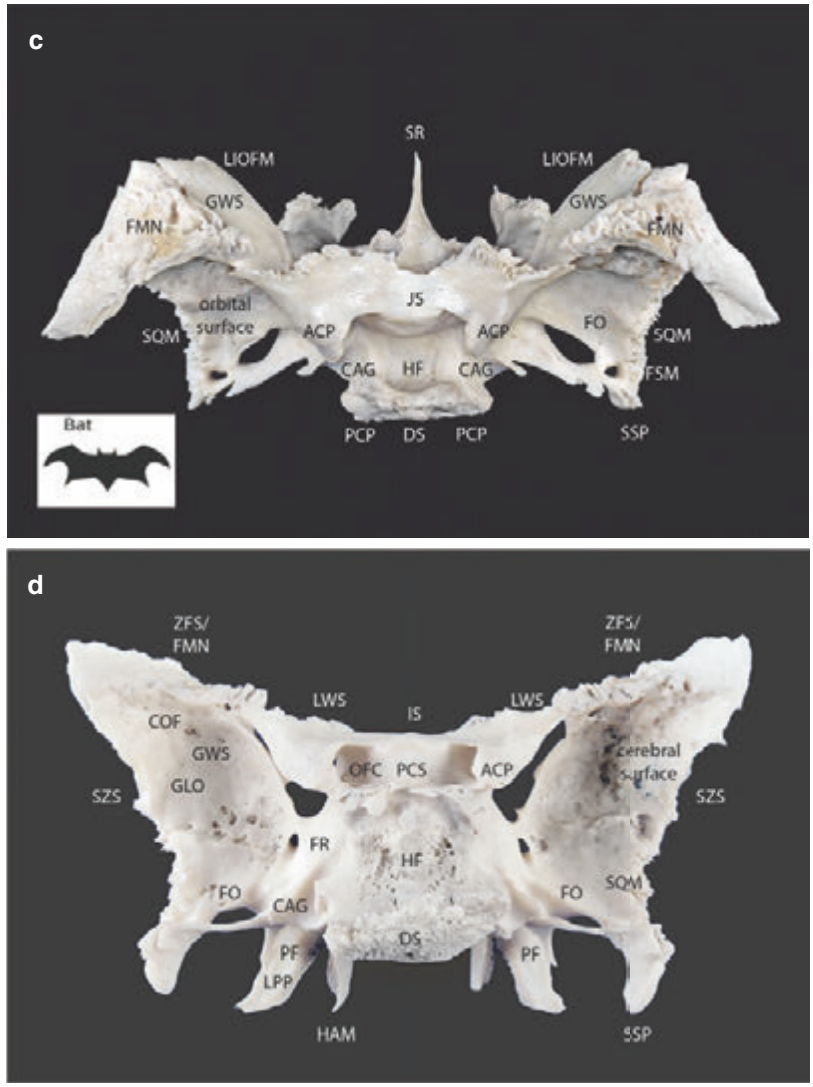

Fig. 2.2 (continued)

Its front view silhouette has the appearance of a wasp (Fig. 2.2a). Because of this appearance, a common term for it was "sphecoid" bone, according to Ancient Greek σφήξ (sphḗx ≈ "wasp" or "hornet") which was used every now and then from the beginnings of medical science in Greco-Roman antiquity until the nineteenth century. The tale (historically unconfirmed) is still bandied that the c in sphenoid was erroneously confused with an *n* resulting in sphenoid which has the meaning of σφην (sphēnoeid ≈ "wedge") in the publishing process of an anatomy textbook and never set right again since then [3, 4]. The triangular lesser wings (alae minores) of the sphenoid (LWS) extend from the superolateral aspect of the body to form the upper border of the superior orbital fissure (SOF), the most posterior part of the orbital roof, and the posterior ridge of the floor of the anterior cranial fossa on either side (Fig. 2.2a). The greater wing (ala major) of the sphenoid (GWS) separates the orbit from the middle cranial fossa and is part of the vertical pterygomaxillary buttress. Each GWS is attached on the lateral aspect of the body by a radix (root). The GWS can be conceived as assembled of three divisions (anterolateral/posterolateral/inferior) which are arranged along and below a vertical compact pillar with a triangular horizontal cross section, nowadays called the sphenoid door jamb (SDJ see later). It ensues a complicated 3-dimensional configuration of two adjacent corners

exhibiting several external and cerebral (internal/endocranial) surfaces. The external medial surface of the anterolateral division corresponds to the plane posterior portion of the lateral orbital wall. The external lateral surface of the same division is docked close to its anterior border at a T-junction by the posterolateral division. The external surfaces of both the anterolateral and posterolateral divisions blend to form parts of the concave medial boundary of the temporal fossa and the external lateral orbital wall. The inferior GWS division spreads underneath the other two divisions starting posteriorly from their vertical intersection (Fig. 2.2c, d). The upper surface of the inferior division conforms to the floor of the medial cranial fossa which is bordered anteriorly and laterally by the cerebral surfaces of the vertical GWS divisions moreover. The bottom surface of the inferior GWS division circumscribes the infratemporal fossa. Axial cross sections unveil the posterior GWS as a central trigone with a spongious bony space between the orbital, temporal, and cranial cortical surfaces (Fig. 2.15b). This potential space for surgical decompression is termed the sphenoid door jamb (SDJ). The superior orbital fissure (SOF) is a gap between the LWS and the GWS. The lower end of the SOF is bounded by the maxillary strut; this is a bony bridge across the foramen rotundum and integral part of the upper GWS radix. The paired pterygoid processes project bilaterally from the inferior aspect of the sphenoid body and its connection to the GWS downwards. It is the base of the lateral pterygoid plate (lamina) that fuses with the root of the GWS in a longitudinal direction. The medial and lateral pterygoid plates band together along the upper portion of their anterior delineations to form the posterior concavity of the pterygopalatine fossa (PPF). The anterior bottom portions of the pterygoid plates remain set asunder forming the pterygoid notch. The notch gap is interposed by the solid inferoposterior end (pyramidal process) of the perpendicular plate of the palatine bone. The suture line arrangements differ and are collectively addressed as the pterygopalatine fissure.

The pterygoid fossa is the vertically oriented open recess between the pterygoid process plates viewed from the posterior aspect. The sphenoid connects to all of the other cranial base bones (Fig. 2.3) and to all bones of the facial skeleton except for the lacrimal and nasal bones.

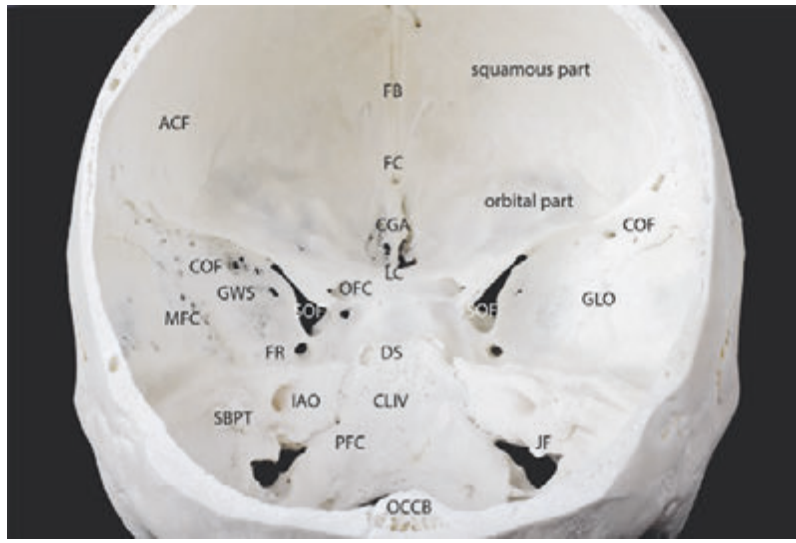

Fig. 2.3 Sphenoid within the cranial fossae—Endocranial surface view. Skull pitched downward posteriorly to bring the OFC, SOF, and Foramen rotundum into view. COF left > right. Note: foramen caecum (FC), crista galli (CGA), and cribriform plate (LC); bony spicule on the floor surface of the anterior cranial fossa. Identify Pterion region inside skull and groove in the lateral orbit (GLO—[2]). The sphenoid entity made up of the body, orbital apices, GWS, LWS, and PPs assumes the role of a backbone that defines the spatial relationships at the transition from the face to the cranial base. *ACF* anterior cranial fossa, *CLIV* clivus, *FB* frontal bone, *IAO* internal acoustic opening, *JF* jugular foramen, *MCF* middle cranial fossa, *OCCB* occipital bone—internal protuberance, *PFC* posterior cranial fossa, *SBPT* superior border of petrous part of temporal bone

Bony Orbital Apex—A Three-Walled/Tetrahedron Spire

The orbital apex within the sphenoid bone needs an elaborated description.

So far there is no unanimously consented definition of the sagittal extent of the orbital apex [5]. For the purposes here, it is regarded as the most posterior projection of the orbital cavity that starts in front of the level of the maxillary strut or foramen rotundum with a narrow triangular base in the frontal cross section (Fig. 2.4a, b) and ends with a pointed tip within the openings of the optic foramen or SOF, respectively. The roof side of the orbital apex is formed by the LWS, the medial side bordered by the lateral surface of the sphenoid body, and the lateral side adjoined by the GWS. The orbital floor with the orbital surface of the palatine bone at its posterior portion comes to a halt at the posterior (rear) IOF sinkhole and does not reach into the orbital apex (Fig. 2.4a, b). In general, two openings can be distinguished within the orbital apex, the optic foramen (OF) representing the intraorbital end of the optic canal and the SOF. The optic strut (OS) constitutes the inferolateral wall of the OC and separates the latter from the SOF (Fig. 2.5a, b).

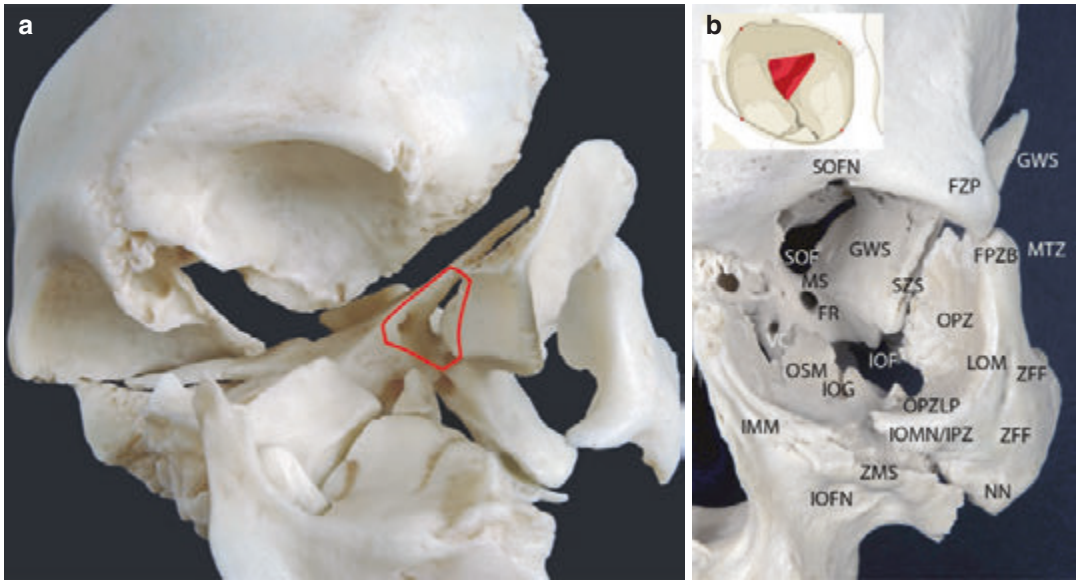

Fig. 2.4 (**a**) Exploded model of the left orbit. Red color marking of the orbital apex which is three-walled spire in contrast to the four-walled pyramid conforming the mid-orbit and anterior orbit. (**b**) Left orbit—Anterior view. Sutures disrupted, palatine, and ethmoid bones removed to spotlight the triangular orbital apex in the back and to expose the posterior (rear) IOF sinkhole. Inset (upper left corner): Geometric outline of the orbital apex. *LOM* lateral orbital margin, *FZP* fronto—zygomatic process, *IOMN/IPZ* infraorbital margin/infraorbital process of zygoma, *NN* nomen nominandum, *ZFF* zygomaticofacial foramen, *ZMS* zygomatico—maxillary suture. (Inset with permission from https://surgeryreference.aofoundation.org. Copyright by AO Foundation, Switzerland)

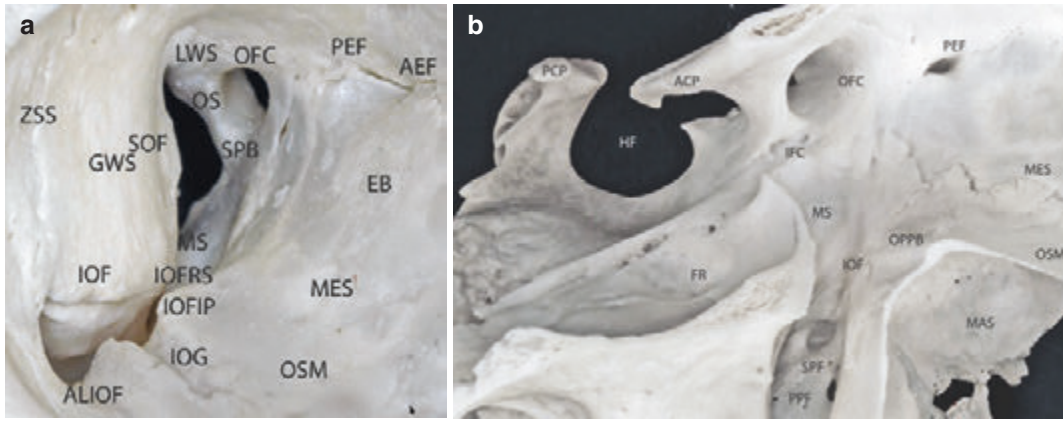

Fig.2.5 (**a**) Architecture of the entire orbital fissure system (right—capital "L"—mirrored image. (—for unmirrored L on the left side—see Fig. 2.4b) extending into the orbital apex and optic canal—anterior close-up view of the major bony pathways in and out of the orbit. *ALIOF* anterior loop of inferior orbital fissure, *EB* ethmoid bone, *IOFRS* inferior orbital fissure rear sinkhole, *IOFIP* inferior orbital fissure isthmus promontory, *MES (~ IOS)* maxilloethmoidal suture line (~ inferomedial orbital strut), *SPB* sphenoid body. (**b**) Junction of orbital apex and lateral sellar region/middle cranial fossa (right)—lateral view. The infraoptic groove (sulcus), tubercle, or canal is the origin of the common annular tendon (Zinn's ring). *IFC* infraoptic canal, *MAS* maxillary antrum/sinus, *OPPB* orbital plate of orbital process of palatine bone, *SPF* sphenopalatine foramen

Frontal Bone—Orbital Roof Constituents

The unpaired frontal bone features external and cerebral surfaces on the sides of a large squamous vertical forehead part (squama frontalis), a nasal part, and two horizontally oriented orbital parts. Each orbital part passes backward behind the supraorbital rim and configures the superior wall (roof) of the orbit in unison with the floor of the anterior cranial fossa to a major extent (Fig. 2.6). The posterior margin of the orbital part articulates with the LWS, which forms a minor most posterior roof portion congruous with the roof of the apex. The posterolateral orbital part margin connects with the upper edge of the GWS along the sphenofrontal suture line (Fig. 2.7). The anterolateral orbital part brings up the zygomatic process and joins with the orbital plate and the temporal process of the zygoma along the frontozygomatic suture line. The orbital roof has the outline of an isoceles triangle that bends up into a concavity. The lacrimal fossa is a shallow depression in the anterolateral roof for the lacrimal gland. The trochlear fovea conforms to the anteromedial adherence zone of trochlear fiber condensations.

The ethmoidal notch is a cove-like slot in between the two orbital plates with a quadrilateral outline, from an endocranial view it is located in the central region of the anterior cranial fossa. Anteriorly the frontal notch turns into the nasal process of the frontal bone (frontal beak) with a serrated margin on either side of the superior nasal spine, a sharp downward process in the midline. The nasal margins articulate with the nasal bones and the frontonasal maxillary processes. The anterior and superior borders of the lacrimal bone connect to the frontonasal maxillary process and to a small strip of the notch margin just behind its anterior corner. In the intact, articulated cranium the interorbital slot is filled by the cribriform plate and the crista galli of the ethmoid bone. The margins of the notch contain several partially opened sinus cells, which have their counterparts in the upper surface of the ethmoid. The sandglass- or two-funnel-shaped fron-

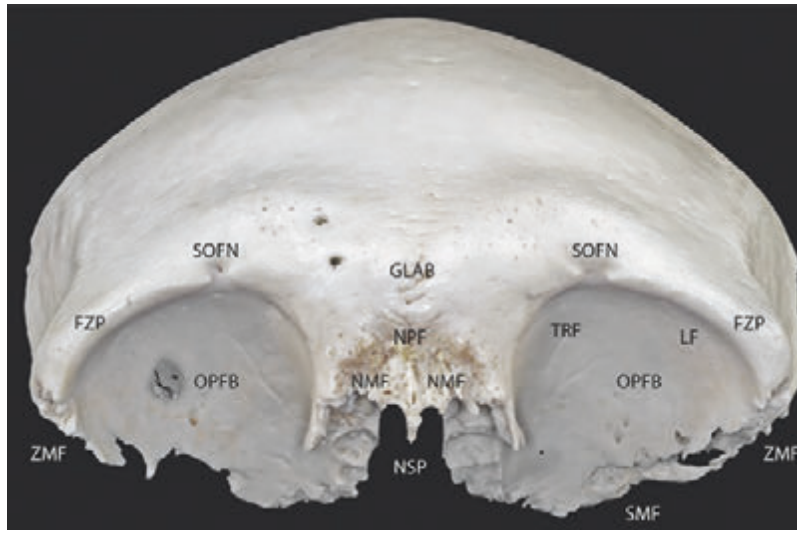

Fig. 2.6 Frontal bone—Anteroinferior view. Orbital surfaces and orbital rims are passing backward. Nasal margin roughly serrated with nasal spine situated medially. Supraorbital openings shaped as notches; Ethmoidal notch bordered with roofs of ethmoidal air cells. *GLAB* glabella, *LF* lacrimal fossa, *NMF* nasal margin of frontal bone, *NPF* nasal part of frontal bone, *NSP* nasal spine, *SMF* sphenoidal margin of frontal bone, *TRF* trochlear fovea, *ZMF* zygomatic margin of frontal bone

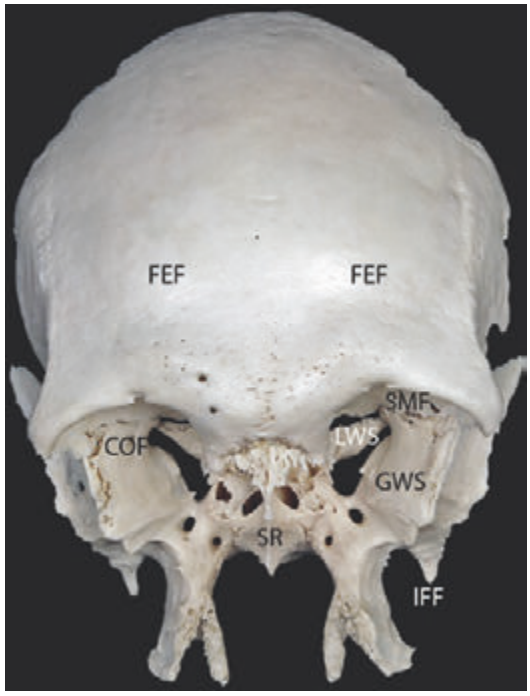

Fig. 2.7 Articulation of frontal bone and sphenoid—Anterior view. The orbital roof is built up including the LWS. The GWS provides the posterior part of the lateral orbital wall. *FEF* frontal eminence of frontal bone, *IFF* infratemporal fossa

tonasal communication and drainage tract presents with an isthmus (frontal ostium) caudal to the bottom of the medial floor of each sinus. The cranial funnel of the tract is accommodated within the confines of the anterolateral notch margin and proceeds further downwards in the niches between the nasal margins and the superior nasal spine to reach into the frontal recess or the ethmoidal infundibulum [6–8]. The extensions of the frontal sinus over the orbital roofs and behind the squamous part of the frontal bone can be intensively pneumatized. The two tables of bone can be extremely thin and may contain dehiscences, so that the periorbita in the roof is in direct contact with the dura mater. The aeration patterns of the frontal sinus show great gender and interindividual variations in number, dimensions, outline, symmetry, septation, and laterality.

The superior orbital wall (roof) to its greatest extent consists of the orbital part of the frontal bone (Fig. 2.8). The most posterior minor portion at the apex is formed by the lesser wing of the sphenoid. The orbital roof takes a triangle shape bent up into a dome.

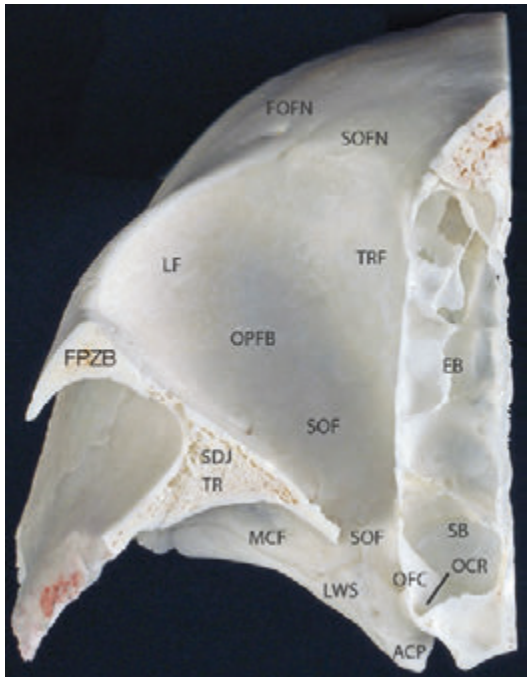

Fig. 2.8 Orbital roof (right) – Inferior view. *OCR* opticocarotid recess, *SB* sphenoid bone, *SDJ* sphenoid door jamp, *TR* trigone (GWS)

Ethmoid, Lacrimal Bone and Frontonasal Maxillary Process—Constituents of the Medial Orbital Wall

The medial wall of the orbit is part of the centrofacial or naso-orbito-ethmoido-nasal unit. It is built up by the sphenoid, ethmoid, lacrimal bone, and the maxilla in a posterior to anterior order (Fig. 2.9).

The lateral wall of the sphenoid body is lined up in front with the lamina papyracea, the paper-thin orbital plate of the ethmoid, and the lateral surfaces of the lacrimal bone and the naso-frontal maxillary process (NFP). The unpaired ethmoid (ethmoidal bone) is located between the two orbits. It contains the ethmoid sinus cells and is forming parts of the nasal and the orbital cavity. The ethmoid bone is built up of the perpendicular plate along the sagittal plane with the crista galli at the upper end (Fig. 2.10a–e). The perpendicular plate corresponds to the bony nasal septum. The cribriform plate extends on each side of the upper perpendicular plate margin in kind of the bar of a T-beam profile. The ethmoidal labyrinths refer to honeycomb arrays of small air cells hanging downwards from the lateral bounds of the cribriform plates. The ethmoidal air cells vary in number and volume on each side and extend in the orbital (i.e., edges of the ethmoidal notch) and squamous part of the frontal bone (Fig. 2.11), occasionally into the sphenoid and into frontonasal process of the maxilla, too. The paramedian portions of the cribriform plate form the roof of the nasal cavity. The rudimentary supreme, the superior, and the middle nasal turbinates (conchae) go down from the medial side of each labyrinth. The boundaries of an ethmoidal labyrinth are often reviewed for didactical illustration in analogy to the sides of a matchbox cover standing on its small longitudinal side (Fig. 2.10a). The box cover is closed posteriorly with the frontal surface of the sphenoid body. In addition to the already open anterior entrance the bottom side of the box is absent in accordance to the open sides of the middle nasal meatus. The lateral wall of the box represents the orbital plate, which is identical with the large rectangular center piece of the medial orbital wall. The orbital plate is paper-thin (lamina papyracea) and transparent, so that the contours of ethmoidal air cells become visible through it (Fig. 2.12). The lower lateral wall of the box or in other terms the inferior ethmoidal cells are adjacent to the medial roof side of the maxillary sinus. The medial wall of the labyrinthine box corresponds to the upper and middle turbinates in alignment at the lateral wall of the inner nose (turbinal wall). The curved basal (ground) lamellae of the superior and middle turbinates fuse with each other and intermingle with the air cell septa network buttressing the paper plate medial orbital wall. The basal lamina of the middle turbinate also reinforces the maxilloethmoidal suture resulting in a firm bony thickening,

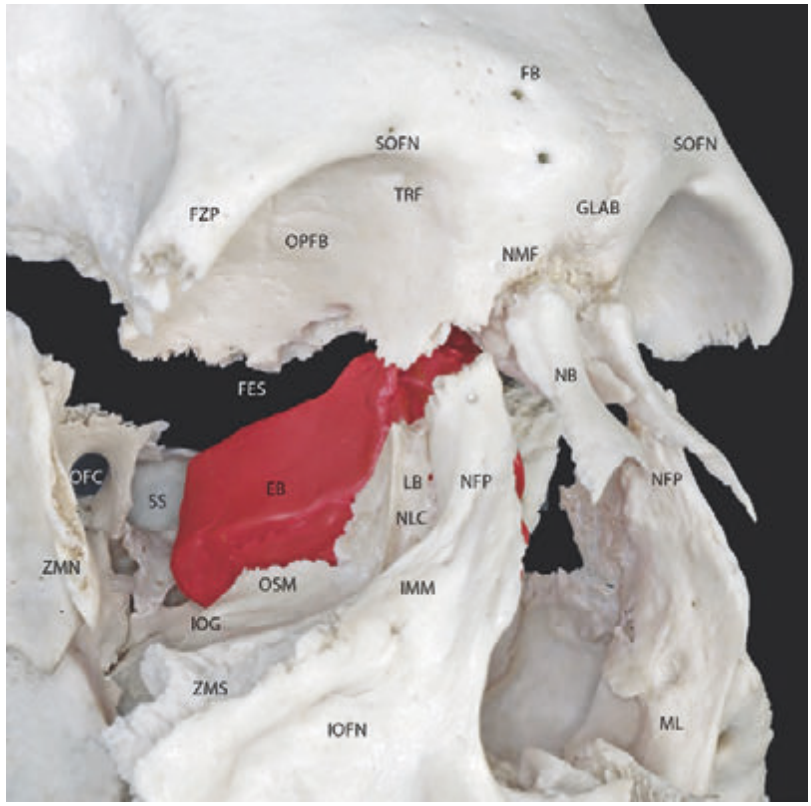

Fig. 2.9 Bony constituents of the right medial orbital wall—Right inferolateral view. The ethmoid (red colored) with the lamina papyracea makes up the large center part of the ensemble of the sphenoid, ethmoid, lacrimal bone, and frontonasal process of the maxilla. *ML* maxillary line, *NB* nasal bone, *NFP* nasofrontal process of maxilla, *NLC* nasolacrimal canal, *SS* sphenoid sinus, *ZMN* zygomatic margin

which is referred to as the inferomedial orbital strut (IOS) (Fig. 2.24a, b).

Clinical Implications

Significance of morphologic properties of the medial orbital wall:

Few and large-volume ethmoidal air cells extending over larger areas of the lamina papyracea are supposed to predispose more fracture susceptibility of the medial orbital wall, in contrast to a high-density reinforcing honeycomb structure [9].

The small trapezoidal lacrimal bones have a nasal and an orbital surface. They are located right in front of the orbital plate of the ethmoid and close to the medial orbital wall across the nasofrontal maxillary process (NFP). Concurrently, they complete the lateral wall of the anterior ethmoidal cells and are part of the lateral wall of the nose where this is overlying the tip of the middle turbinate. A vertical ridge, the posterior lacrimal crest, protrudes along the orbital surface and divides it into a smooth plane posteriorly and into a carved out longitudinal groove (lacrimal sulcus). The anterior margin of this sulcus joins to the likewise grooved posterior margin of the NFP and completes the entrance into the nasolacrimal canal. The orifice at the initial canal section is widened and creating a fossa for the lacrimal sac. The upper lateral slope of the NFP carries the anterior lacrimal crest in parallel to the anterior circumference of the canal inlet zone.

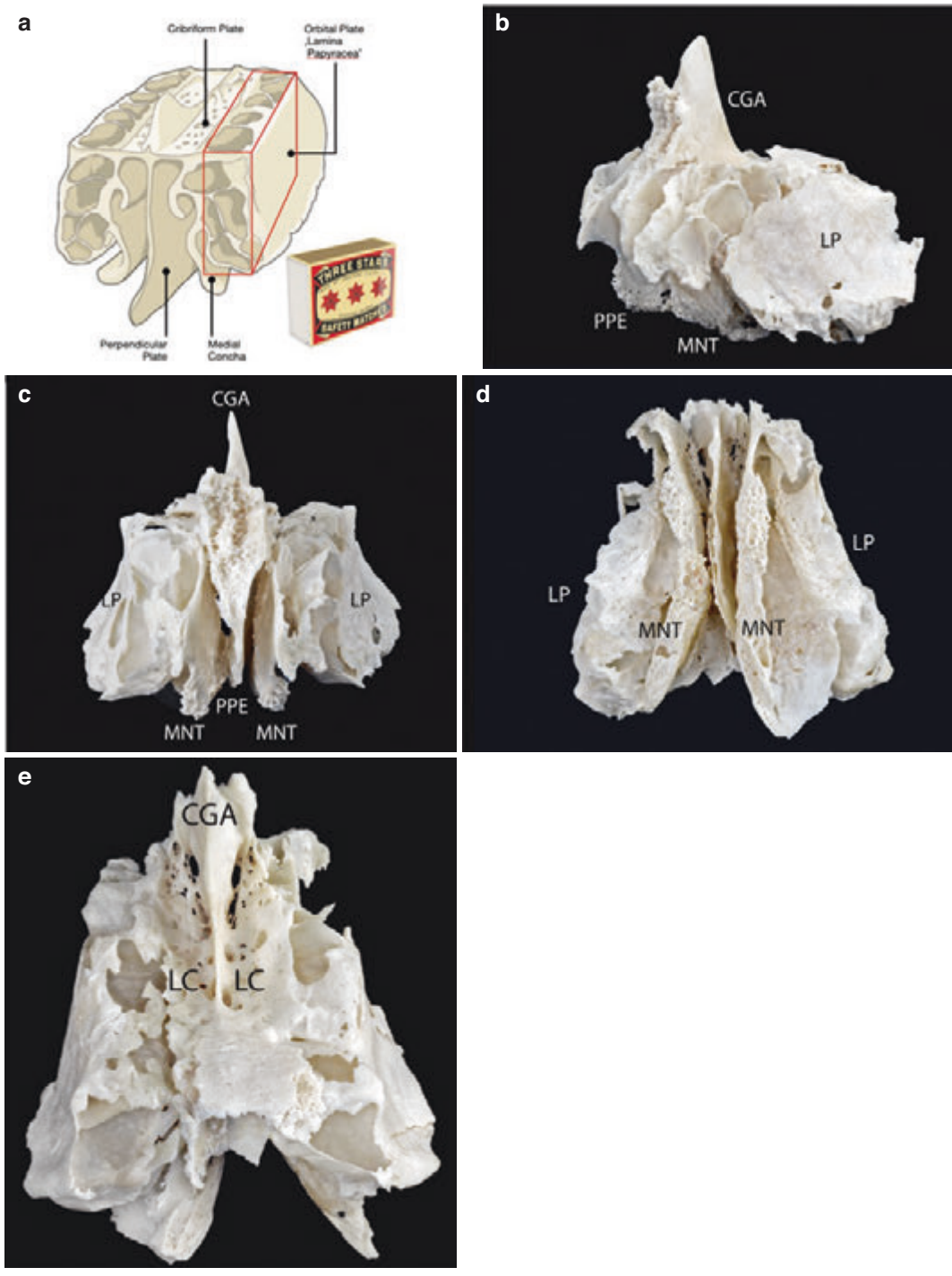

Fig. 2.10 (**a**) Graphic layout of the ethmoid—Left anterolateral view. Illustration of main components. Red contour silhouette indicates geometry of an ethmoidal labyrinth. Inset: Matchbox comparison to review the surfaces of a labyrinth (see text). (Ethmoid sketch with permission from https://surgeryreference.aofoundation.org). (**b**) (Upper right): Ethmoid—Left anterolateral view. Bony analogue to Fig. 2.9. Note: Anterior and middle ethmoidal air cells with open roof. *LP* lamina papyracea, *MNT* middle nasal turbinate (Concha), *PPE* perpendicular plate of ethmoid. (**c**) (Middle left): Ethmoid—Posterior view. Note: Posterior ethmoidal air cells open. (**d**) (Middle right): Ethmoid—Inferior view. (**e**) (Low): Ethmoid—Posterosuperior view. Labyrinthine air cells with open roofs. *LC* lamina cribrosa/cribriform plate

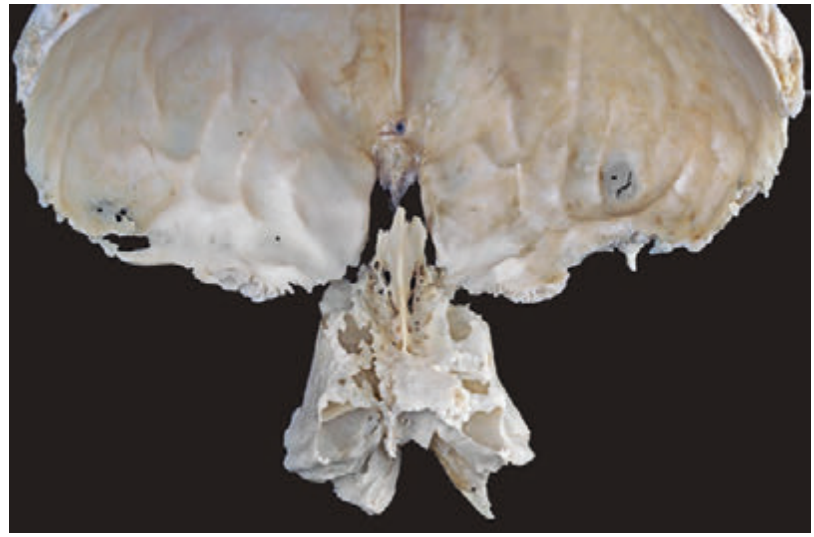

Fig. 2.11 Frontal and ethmoid bones—Frontal and ethmoid bones from superior view showing the upper cerebral surfaces. Articulation assembly. The ethmoid air cells are capped by apposition with the roofs of the ethmoid notch edges

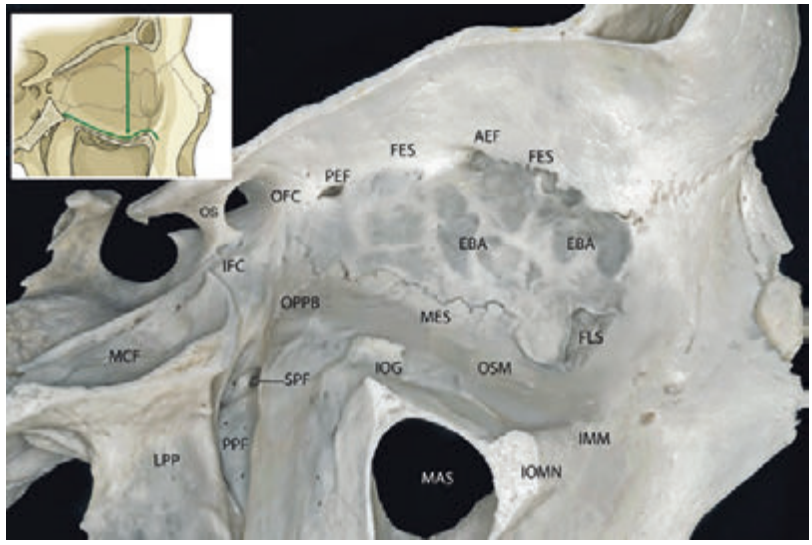

Fig. 2.12 Medial orbital wall—lateral to medial view offering a look into the OFC and the pterygopalatine fossa along the medial IOF margin and retrotuber maxillary region. Inset (upper left corner)—Vertical extent of the postentry zone. Behind the infraorbital and supraorbital rim (vertical green arrow). Lazy-S shape of ascending orbital floor - undulation allusive only (green line). *EBA* ethmoid bone/air cells, *LPP* lateral pterygoid plate. (Inset with permission from https://surgeryreference.aofoundation.org)

The posterior lacrimal crest may be elongated together with a small portion of the lower smooth plane into a hooked process. This lacrimal hamulus interdigitates with a corresponding notch of the NFP at the caudal periphery of the canal entrance.

Palatine Bone and Maxilla—Major Constituents of the Orbital Floor

The palatine bone is interposed between the back of the maxilla and the base as well as the medial and lateral plates of the pterygoid process (Fig. 2.13a). It

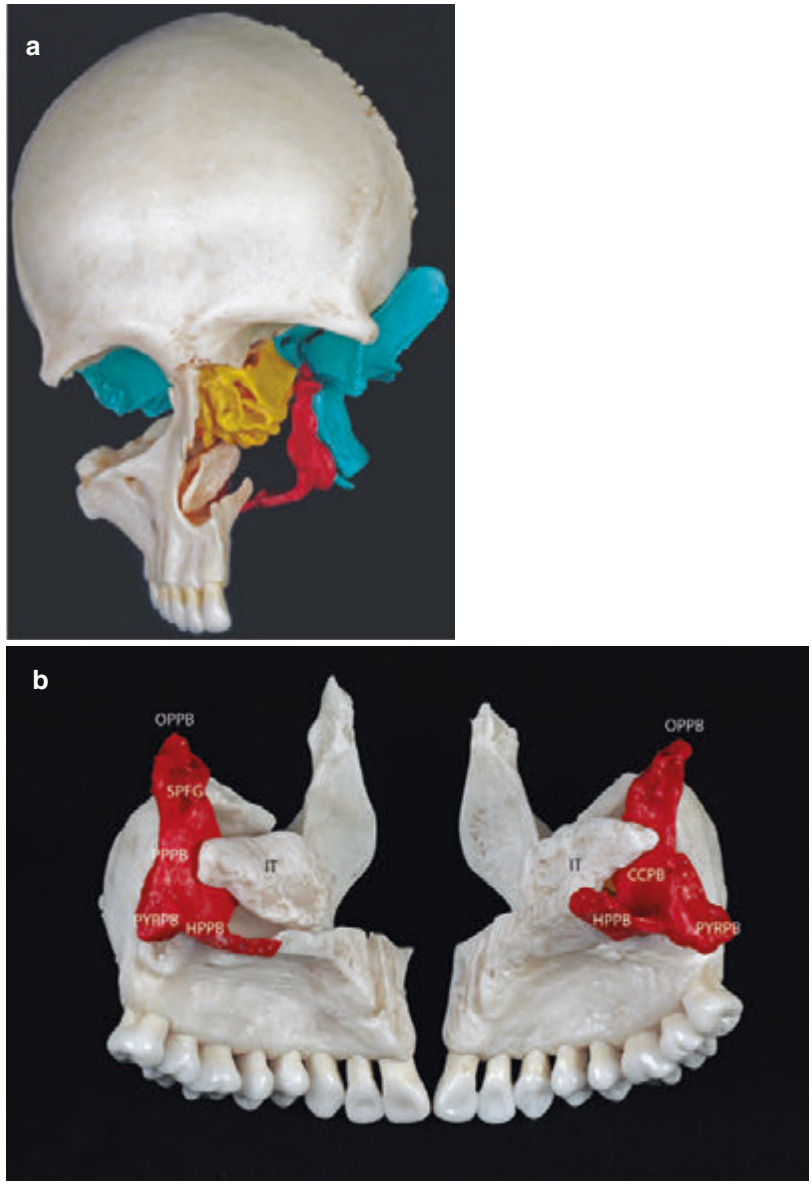

Fig. 2.13 (**a**) Osseous model set up demonstrating the origin of the posterior ledge—the orbital process of the palatine bone (red) is the rearmost portion of the orbital floor with its orbital plate ('facies orbitalis'/OPPB) (= posterior ledge), it is contiguous to the upper end of the perpendicular plate. Ethmoid bone (yellow), sphenoid (turquoise) with GWS, LWS, and pterygoid process—outer lamina and hamulus. (**b**) Posterior view of the maxillae (swung out) to appreciate the orbital process of palatine bones (red) as robust constituent of the posterior orbital floor. *CCPB* conchal crest of palatine bone, *HPPB* horizontal process of palatine bone, *IT* inferior turbinate, *PPPB* perpendicular process of palatine bone, *SPFG* sphenopalatine foramen/groove. (**c**) Right palatine bone—view from the front. *OPPB* orbital process of palatine bone, *PYRPB* pyramidal process of palatine bone, *SPNPB* sphenopalatine notch (palatine bone), *SPPB* sphenoidal process of palatine bone. (**d**) Right palatine bone—view from above in anteroposterior orientation. *PNS* posterior nasal spine. (**e**) Pair of isolated palatine bones oriented in an oblique antero-posterior direction resembles antlers. The smooth surface of the orbital plate at the top of the right orbital process (OPPB) breaks off at a distinct edge posteriorly and converges into the front wall of the rear sink of the inferior orbital fissure (IOFRS). MPPB, Maxillary Process of Palatine Bone; GPG, Greater Palatine Groove. OPPB Detail–Inset (upper right corner): edged demarcation line between the posterior end of orbital floor and IOF rear sink (green line grid) surfaces

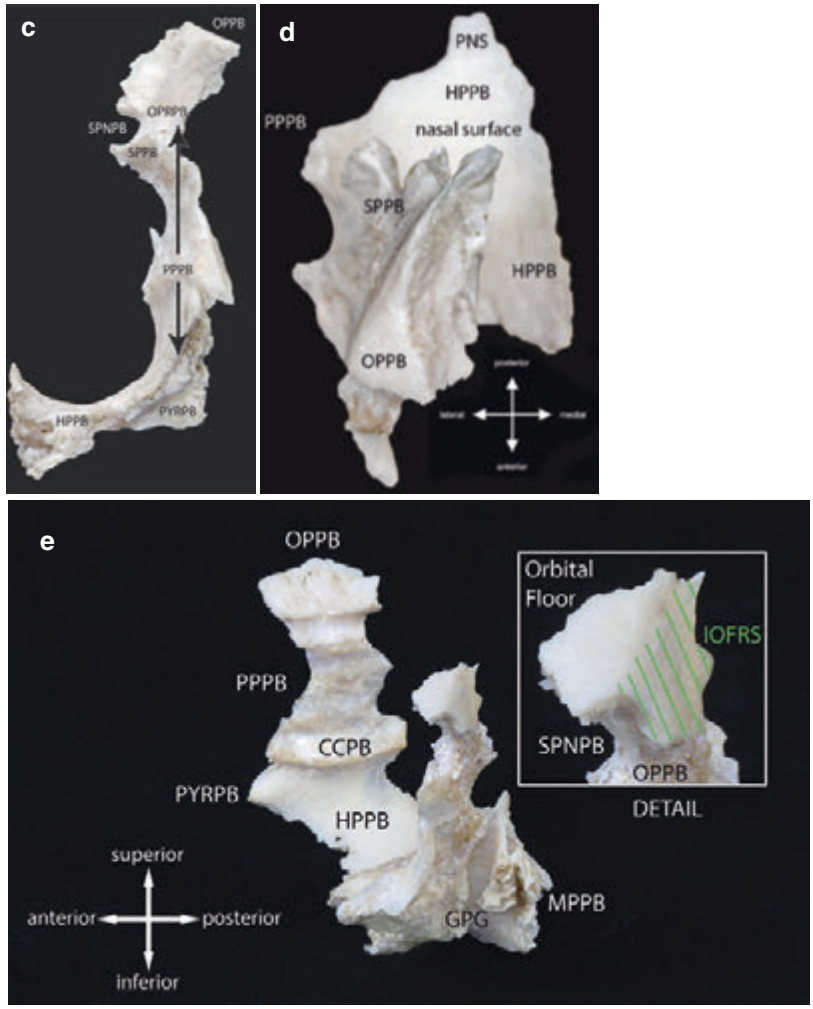

Fig. 2.13 (continued)

contributes to the posterior lateral wall of the nasal cavity, the hard palate, the PPF, and the orbital floor in an intriguing configuration. Basically, the palatine bone consists of a vertical part (perpendicular plate) with a medial oblique orientation and a horizontal part or plate providing the posterior hemihard palate portion. The upper end of the perpendicular plate is overtopped by the orbital and sphenoidal processes. The orbital process of the palatine bone (OPPB) is situated at a higher level than the sphenoid process and projecting anterosuperiorly. It is based on a neck narrowed by the half-oval sphenopalatine notch (SPNPB) at the posterior aspect which also sets it apart from the sphenoidal process that is attached at the inferior margin of the notch and diverges medially and upwards. The orbital process presents with five surfaces in total. The anterior surface connects with upper medial end of the posterior surface of the maxilla. It is common to refer to the superior surface of the orbital process of the palatine bone, as to the orbital plate of the palatine bone (OPPB) more briefly. The OPPB is triangular in shape and sloping slightly upwards in combination with a downward tilting laterally (Fig. 2.13b–d). Since the OPPB conforms the rear end of the orbital floor, that is often preserved in defect fractures and may serve as support in surgical reconstruction therefore, it is simply addressed as the "posterior ledge" in surgical jargon. The remaining three surfaces are directed either posteriorly to abut the anterior sphenoid body, or medially to join with the ethmoid and laterally toward the pterygo-

palatine fossa (PPF). The orbital process may enclose an air cell, which is open either to the sphenoid sinus, the posterior ethmoidal cells or with both at once [10–12]. The sphenoidal process attaches to the medial base of the pterygoid process. The anterior border of the sphenoidal process bounds the posterior SPNPB margin, while the anterior notch margin is molded by the posterior neck of the orbital process (OPPB).

The sphenopalatine foramen (SPF) has a posteromedial angulation to the sagittal plane. The SPF results from the union of the inferior surface of the sphenoid body with the superomedial marginal SPNPB circumference. The communication between the PPF and the posterior nasal cavity is via the SPF. In topographical relations, the bony SPF surroundings form the medial wall of the posterior (rear) IOF sinkhole and the vertically oriented surface descending from the posterior OPPB border.

Clinical Implications

The position of the posterior ledge in terms of linear distances between the infraorbital margin above the infra-orbital foramen and landmark points at the OPPB, the anterior SOF and ventrolateral entrance of the OFC has been assessed in a CT-based cohort study as a guideline for the safe surgical approach in the repair of inferomedial orbital wall fractures [13].

The potential of an OPPB resection for expansion of the surgical corridor in the endoscopic approach to the orbital apex has been checked in a morphometric analysis of the area dimensions in macerated skulls [14].

The orbital surface of the maxilla (OSM) makes up the largest part of the orbital floor [15]. It is the upper of a total of four surfaces of the body of the maxilla (corpus maxillae) which contains the maxillary sinus or the antrum (of Highmore), respectively. Hence, the OSM is also the ceiling of the antrum. The outline markings of the orbital surface fit a smooth triangular plate, which has an inclination angle of 45° to the horizontal plane. The posterior OSM border converts into the rounded anteromedial IOF margin and its consecutive vertical wall, which is interchangeable with the infratemporal surface of the maxillary body. At its front, the anterior OSM blends into the infraorbital margin (IMM). The IMM extends into the lower part of the medial orbital margin (MOMLP) and further on into the nasofrontal maxillary process (NFP). Laterally, the IMM terminates with the zygomatic process. The lower part of the medial orbital plate of the zygoma (OPZLP) provides a small anterolateral flange to the orbital floor just behind the lower lateral corner of the rim. A small bony depression behind the lower medial corner of the rim and immediately lateral alongside the nasolacrimal canal is the origin to the inferior oblique muscle.

The NFP has a plate-like shape and is forming part of the sidewall of the nose along the upper lateral border of the piriform aperture. At the cranio-medial end, the NFP articulates with the frontal bone and the nasal bone (Fig. 2.14).

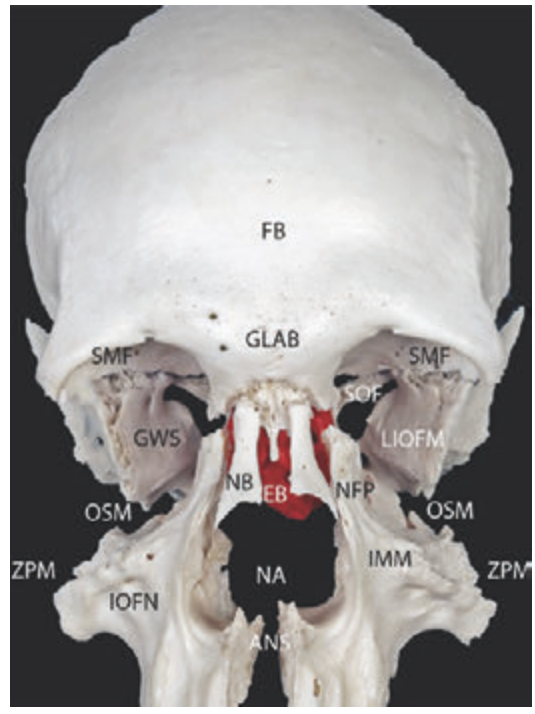

Fig. 2.14 Maxillary building blocks in central midface—Anterior view showing the maxillary processes and relationships to frontal bone, nasal bones, and ethmoid (red colored). *ANS* anterior nasal spine, *NA* nasal aperture, *ZPM* zygomatic process of maxilla

The posterior margin raises the anterior lacrimal crest (ALC) before it transforms into the lacrimal fossa and the entrance into the nasolacrimal groove and canal (NLC), which emanate in combination with the contours and borders of the lacrimal bone.

The zygomatic or malar process is passing laterally for articulation with the zygomatic bone. This process rests on the zygomaticomaxillary crest, a porch jutting out with a slightly arched border from the junction of the anterior and infratemporal surfaces of the maxillary body that extends upward at the level of the first upper molar. The upper surface of this process is a rough and serrated triangular platform that has a downward angulation to the lateral side. The borders of this platform bring up the zygomaticomaxillary suture lines together with the edges of the medial undersurface of the zygoma (Figs. 2.15a, b, 2.16b, and 2.17a, b). The orbital floor is shorter in anteroposterior extent than the three other orbitals walls and thus is missing in the orbital apex (Fig. 2.15a, b).

The posterior or infratemporal surface of the maxillary body covers the curving vertical area between the posterior aspect of the nasal surface to the lateral margin of the zygomaticomaxillary crest (Fig. 2.15c). The maxillary tuberosity is bowing out backward from the lower lateral portion of this surface. A small crescentic rough site at the medial posteroinferior aspect at the junction of the posterior and medial surface is attached to the maxillary process at the lateral surface of the perpendicular plate of the palatine bone. The greater palatine canal is formed by the apposition of two obliquely oriented grooves descending on each side of the bony interface.

The melding seamline along the upper border of posterior surface is the link to the orbital plate and corresponds to the anteromedial IOF margin. This rounded hillslope at the back of the seamline into the IOF rear sinkhole (IOFRS) is engraved by the infraorbital groove (sulcus) [16]. The infraorbital groove (IOG) often begins with a deep U-shaped hollowing in the middle of the posterior maxillary floor. It passes forward over varying distances before it transforms into a canal structure [17]. The infraorbital canal (IOC) moves downwards and gets suspended on a bony beam resembling a mesentery protruding from underneath the orbital floor [18]. This conduit ends in the anterior antral wall usually with a single infraorbital foramen (IOFN). In adults, the foramen is located 7–10 mm below the infraorbital margin and above the canine fossa purportedly on a plumb line passing through the mid-pupil.

Clinical Implications

The position and relative length of the infraorbital groove and canal are supposed to be predisposing factors to the occurrence and pattern of fractures within the orbital floor [19].

The medial or nasal surface is dominated by the maxillary hiatus, a large irregular aperture to the maxillary sinus, which is covered and downsized by the perpendicular plate of the palatine bone posteriorly, the inferior turbinate inferiorly, and the ethmoidal labyrinth—in particular by the uncinate process—together with the lacrimal bone superoanteriorly. The medial OSM border is assembled alongside the maxilla-ethmoidal suture line as part of the inferomedial orbital strut (IOS) and comes up against the lower borders of the lamina papyracea and the lacrimal bone [20]. The two paired maxillae are the largest bones in the midface. Uniting below the nasal aperture at the level of the anterior nasal spine and along the midline of the hard palate, they aggregate to the upper jaw (Fig. 2.14).

Apart from the body including the frontonasal and zygomatic process, there are two other components contributing to the overall architecture of a maxilla, the horizontal palatine process, and the alveolar process curvature. Altogether, these components are involved in the structural organization of the orbital, nasal/paranasal and oral cavities.

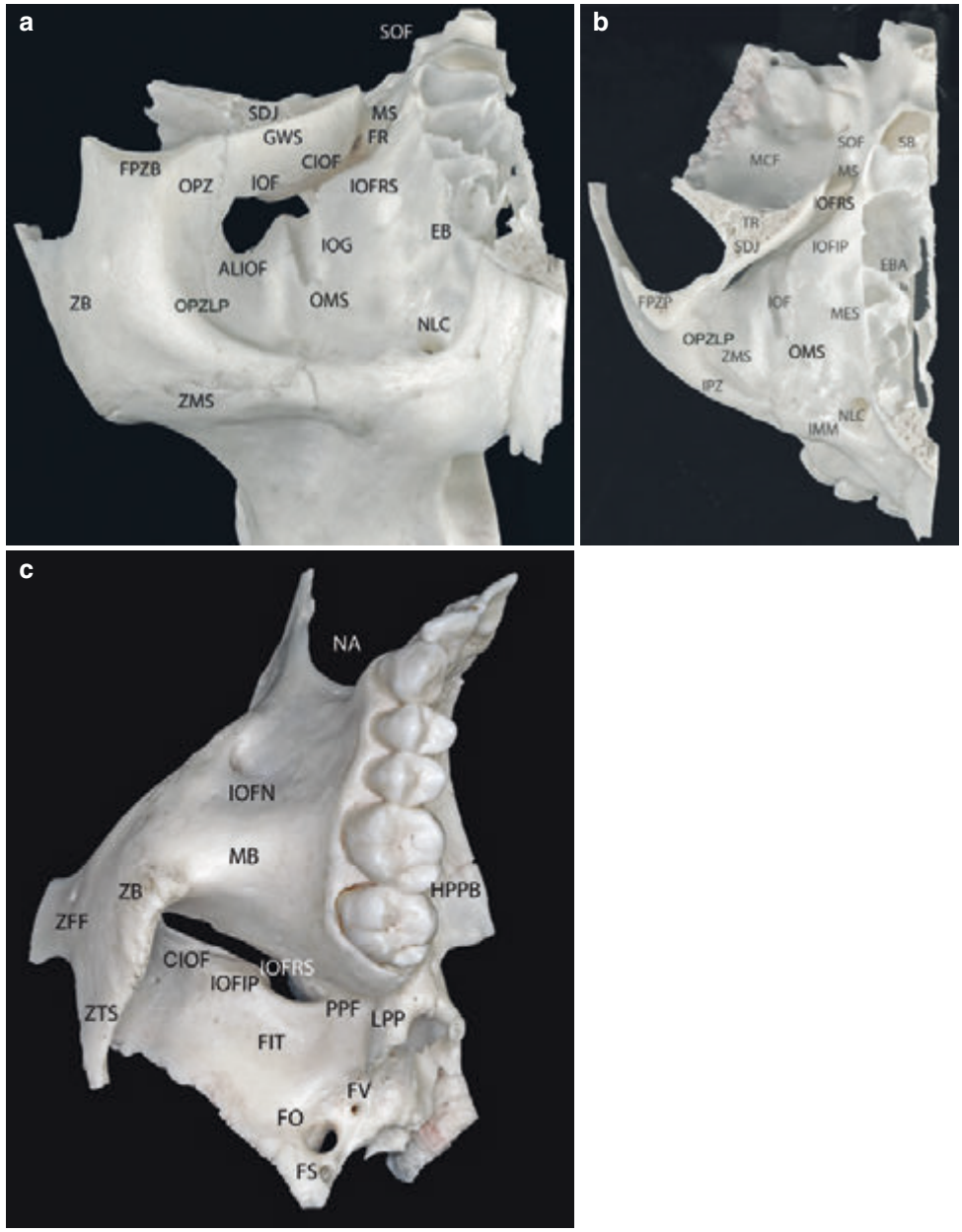

Fig. 2.15 (**a**) Orbital floor (right)—anterocranial view (lower margin tilted forward). The IOF communicates with the infratemporal and pterygopalatine fossa. Rather than a simple punched perforation in a shelf the IOF is configured as a ravine with steep sides, sinkholes, and affluents such as the foramen rotundum, pterygoid canal, and inferior orbital groove. *CIOF* confluence IOF isthmus, *OPZLP* orbital plate of zygoma lower part, *IOFRS* inferior orbital fissure rear sinkhole. (**b**) Orbital floor (right) from above. The posterior end of the IOF ends in a sinkhole in front of the maxillary strut. Thus, the orbital floor does not contribute to the apex (= posterior orbit). nasal/paranasal and oral cavities. (**c**) Assembly of maxilla, zygoma, and sphenoid bone (right)—inferolateral aspect showing retrotubar and infratemporal region. The ravine-like character of the IOF with robust posterior bony borders (TR and medial IOF margin) is confirmed. *FIT* fossa infratemporalis, *FV* foramen vesalii/sphenoidal emissary foramen, IOFIP inferior orbital fissure promontory, LPP lateral pterygoid plate, *MB* maxillary bone, *ZB* zygomatic bone, *ZTS* zygomatica–temporal suture

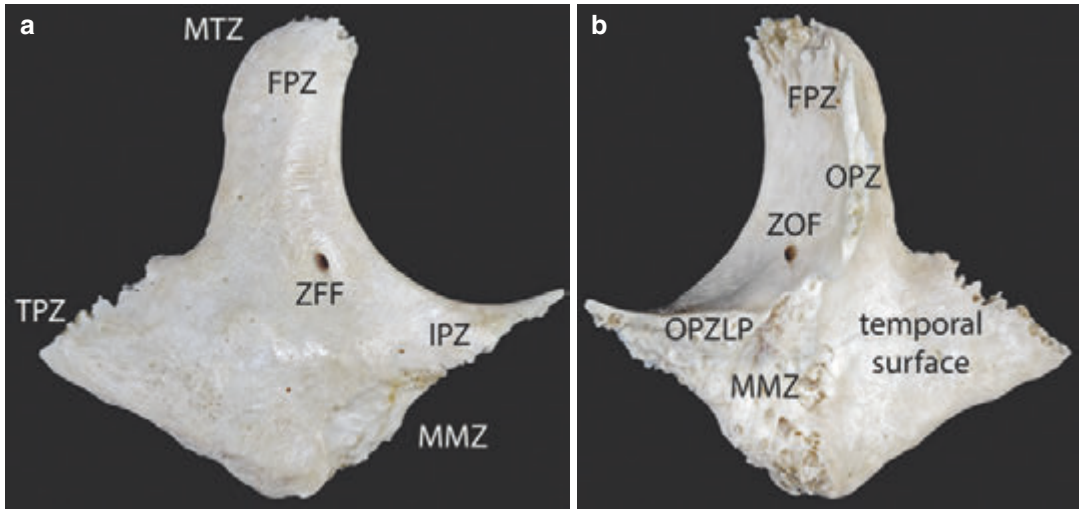

Fig. 2.16 (**a**) Right Zygoma—Lateral view. Convex outer zygomatic surface. Note zygomatic-facial foramen (ZFF) next to the reversal point along the curved margin in the lower lateral orbital quadrant. A slight roll-shaped elevation below the ZFF gives origin to the zygomaticus major muscle. *MMZ* maxillary margin of zygoma, *TPZ* temporal process of zygoma. (**b**) Right Zygoma–Medial view. The two portions of the overall orbital plate, the OPZ and the OPZLP (i.e., the anterolateral orbital floor) divide the orbital surface from the temporal surface along the sphenozygomatic suture line (SZS - see Fig. 2.4b). The rough keel-shaped area, the maxillary margin (MMZ) is part of the broad bony interface with the maxilla (ZPM—see Fig. 2.14), termed the zygomatic-maxillary suture (ZMS) line. *ZOF* zygomatico-orbital foramen

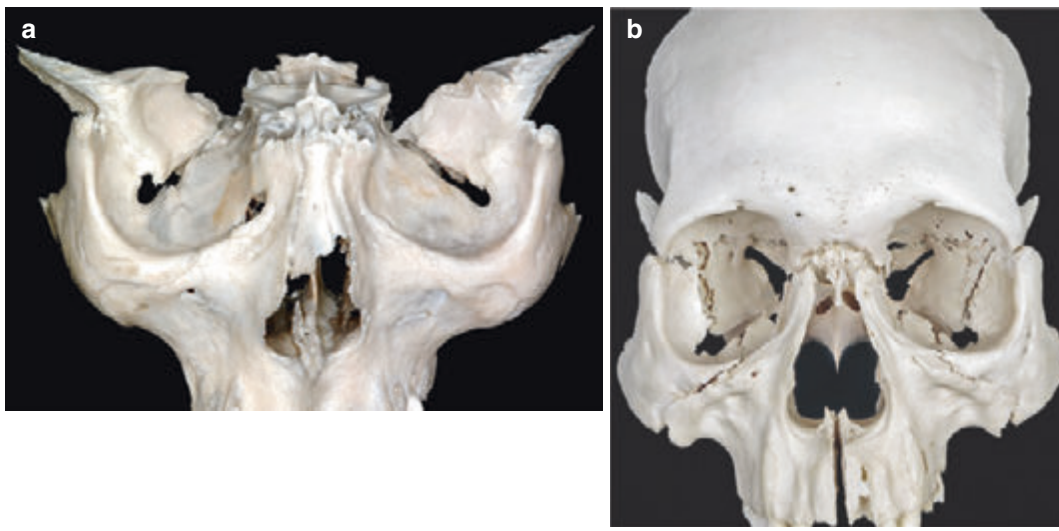

Fig. 2.17 (**a**) Zygomatic bones in closed lock position between sphenoid and maxillae—anterior view of the midface, LWS, and frontal bone removed. Follow the connections along sphenozygomatic suture (SZS) lines and zygomatic-maxillary suture (ZMS) lines/junctions. The anterior IOF loops are interposed in between the OPZ and OPZLP. (**b**) Assembly of midface building blocks completed—Anterior view. Note: Ethmoid, vomer, and palatine bones removed

Zygoma—Constituent of the Lateral Orbital Wall

The zygoma, malar, or cheek bone is the prominent cornerstone of the upper lateral midface (Figs. 2.4b and 2.16a, b). The orbital plate (facies orbitalis) of the zygoma (OPZ) is directed posteromedially at an angle of 45° toward the sagittal plane. In conjunction with the vertical frontal process (FPZ), the OPZ completes the lateral orbital wall and makes up the lateral orbital margin (LOM) including the rim around the lower lateral quadrant. Thereto the OPZ joins up with the anterior GWS border along the sphenozygomatic suture line (SZS) (Fig. 2.17a), while the zygomatic-frontal-suture line (ZFS) is the anterosuperior contact zone between the two according frontal processes from above and below (Fig. 2.17b). Anterior to the massive central trigone of the GWS, the lateral orbital wall turns into a monocortical layer with the SZS line located in the thinnest portion. The indented bay between the margins of the anterior loop of the IOF partitions a small horizontally oriented lower part (OPZLP) from the overall orbital plate. The OPZLP conforms the anterolateral orbital floor (Figs. 2.15a, b and 2.17a, b).

The orbital tubercle or Whitnall's tubercle [21] is a small roundly protuberance of 2 mm or 3 mm diameter on the inner OPZ immediately (2–4 mm) in the marginal territory behind the orbital rim and about 10–11 mm beneath the ZFS. The tubercle gives attachment to the lateral retinacular suspension complex. The marginal tubercle (MTZ) corresponds to a spine at the posterior upper edge of a FPZ widening that is occasionally present somewhat below the ZFS.

The solid zygomatic body has a rhombus shape and exhibits three further extensions in a medial, caudal, and posterior direction. The infraorbital process (IPZ) courses medially, while the adjacent maxillary margin is beveled diagonally downwards and laterally to merge with the tapering inferior tip of the zygoma (malar tuberosity), at last the temporal process reaches out backward to convey into the anterior zygomatic arch. The outer surface of the zygoma is commonly addressed as the malar or oftentimes inappropriately as lateral surface. The inner surface has been summed up as the temporal or infratemporal surface without drawing any clear distinction between the rear sides neither of the orbital plate or frontal process, the zygomatic body, or the temporal process.

A set of foramina with a network of interconnecting zygomatic channels perforates the OPZ as well as the malar and infratemporal surfaces of the zygoma. These foramina show a lot of variations from complete absence to multiplicity [22, 23]. The single or plural orifice(s) of the zygomatic-orbital foramen (ZOF) open(s) at the inner surface of the anterior inferolateral orbital quadrant next to the IOF loop (Fig. 2.15b). The zygomatic-facial foramen (ZFF) is located within the central range of the outer zygoma surface (Fig. 2.16a). The zygomatic-temporal foramen (ZTF) occupies an ascended position behind the frontal process or the zygomatic body.

Clinical Implications

The sphenozygomatic suture line (SZS) is an essential reference and reliable guide in the reduction of the fractured zygoma and consecutively for reestablishing of the outer facial frame. For this purpose, the lateral orbital wall is under intraoperative control from inside the orbit for accurate restoration into a flat continuous plane [24, 25].

Anterior Orbit—Midorbit—Posterior Orbit (Apex)

It is still often used practice to divide the length of the orbit into three-thirds according to the anteroposterior extension. This division is intuitive and not based on acknowledged anatomical references or appropriate metric distances between consented measuring points or planes. The orbital floor which is shorter than the other three walls is often the only zone taken into con-

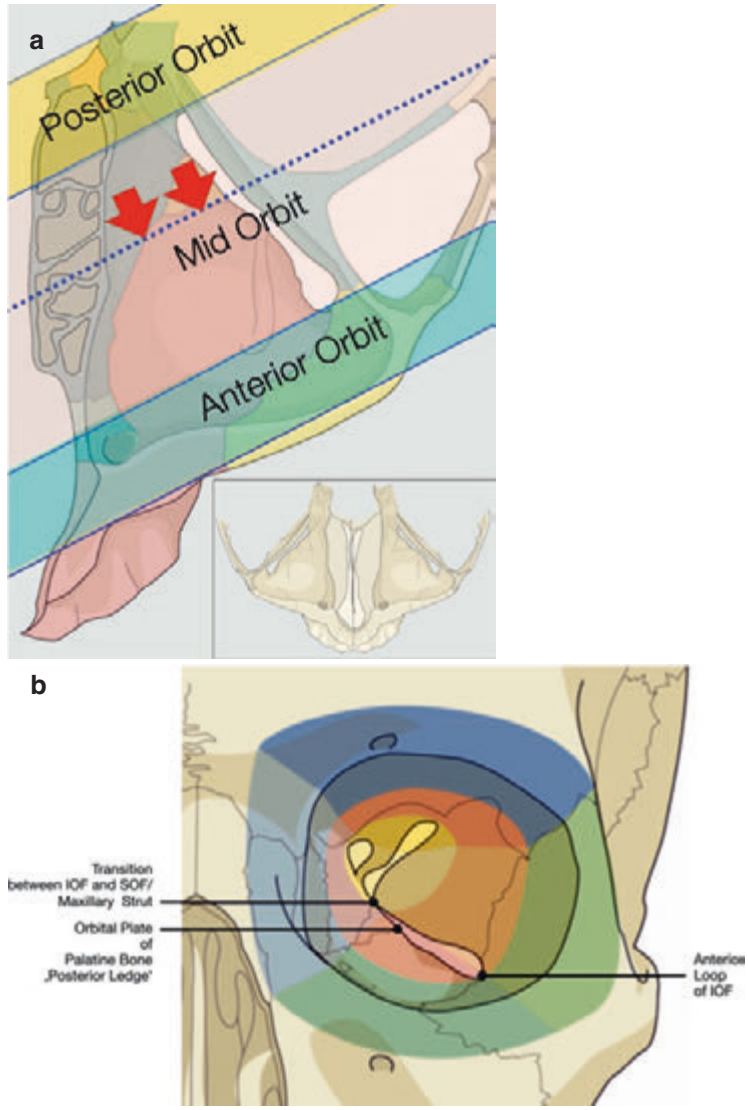

Fig. 2.18 (**a**) Left orbital floor from above—Borderlines between the anterior orbit (blue green)—midorbit (pink) and posterior orbit (yellow) in relation to the IOF. The dotted line indicates altered proportions, if the anterior border of the orbital plate of the palatine process serves as a point of reference. Inset (right lower corner)—orienting view over both orbits. (**b**) Left orbit frontal view—points of reference along the IOF and ensuing concentric. (**a** and **b** with permission from https://surgeryreference.aofoundation.org)

sideration and divided into three parts. Within the perspectives of the entire orbit, this must lead to confusion, since the apex with its triangular cross section is usually regarded as the posterior part, whereas the orbital floor extends over the remaining two thirds of the orbital depth. A more pragmatic approach is the partitioning into an anterior orbit, a midorbit, and a posterior orbit (apex orbitae) based on reproducible anatomic landmarks. The IOF appears most suitable for the provision of reproducible topographic indicators (Fig. 2.18a, b). A frontal plane at the level of a tangent to the tip of the anterior IOF loop provides the boundary between anterior orbit and the beginning of the midorbit. A second frontal plane placed at the transition of the IOF into the SOF anterior to the maxillary strut separates the midorbit from the posterior orbit or the apex orbitae.